CALCULATION OF CLOSED ORBIT ERRORS DUE TO MISALIGNMENT OF COMBINED FUNCTION MAGNETS WITH LARGE BEND ANGLE

Eva S. Bozoki[+]
Brookhaven National Laboratory, Upton, NY, 11973

1. ABSTRACT

The effects of different misalignments of bending magnets with very small bending radius (ρ < 1m) and very large bending angle (Φ_b = 180, in some cases 360°) are discussed. These magnets are represented by n segments. A method is given to calculate misalignments of a segment at any $\alpha < \Phi_b$ bend angle from the misalignments of the whole (rigid) magnet. This method is then used to calculate distorted closed orbits for the SXLS ring.

2. INTRODUCTION

With the advent of the compact electron synchrotons/storage rings, the role of bending magnets of very small bending radius (ρ < 1m) and very large bending angle (Φ_b = 180°, in some cases 360°) are becoming important [1-4]. The horizontal and/or the vertical betatron phase advance can be significant across the magnet. Furthermore, these magnets are combined function magnets having significant quadrupole, sextupole and higher harmonic components in addition to the dipole field.

There are few other magnetic elements in the compact rings, and those elements are relatively short and straightforward to manufacture and to align to great accuracy. Therefore the significant sources of closed orbit errors in the compact rings are the above large bending angle magnets.

3. SOURCES OF ORBIT ERRORS

Kicks along the path of the beam can arize from magnet imperfections (field errors) and magnet misalignments (which result in deviation from the ideal field along the beam path). In case of air-core superconducting magnets the misalignment of the coils can be looked at as "magnet misalignments".

For a $\Psi(s')$, $s_1 < s' < s_2$ extended kick, the resulting closed orbit displacement is

$$\zeta(s) = \frac{\sqrt{\beta(s)}}{2\sin\pi\nu}\int_{s_1}^{s_2} \Psi(s')\sqrt{\beta(s')}\cos[\phi(s) - \phi(s') - \pi\nu]ds', \tag{1}$$

where $\zeta = x_{co}$ *or* y_{co} and β, ϕ and ν are the betatron function, phase advance and tune, respectively. If the phase advance is small along the kick, then it can be treated as a point kick at the middle of the magnet and the integral can be replaced by its value at the point kick location.*

Table-1 lists the field errors and misalignments which can lead to closed orbit errors in the presence of dipole, quadrupole and sextupole field.

--

Table-1
Sources of closed orbit errors

elmt	source	ΔB	$\Psi_{x,y}$	effect
pure	field error, ΔB_y	ΔB_y	$\Phi_b \Delta B_y / B_y$	x_{co}
	field error, ΔB_x	ΔB_x	$\Phi_b \Delta B_x / B_y$	y_{co}
D	displ., Δz	$\Delta B_y = -B_y \Delta z$	$\Delta z / \rho$	x_{co}
I	roll, Θ_z	$\Delta B_x = -B_y \Theta_z$	$\Phi_b \Theta z$	y_{co}
P	pitch, Θ_x	$\Delta B_z = B_y \Theta_x$		x-y coupl
Q	displ., Δx	$\Delta B_y = B' \Delta x$	$K^2 L \Delta x$	x_{co}
U	displ., Δy	$\Delta B_x = B' \Delta y$	$K^2 L \Delta y$	y_{co}
A	roll, Θ_z	$\Delta B_y = -2B' y \Theta_z$		x-y coupl
D		$\Delta B_x = 2B' y \Theta_z$		x-y coupl
S	displ., Δy	$\Delta B_y = -2B'' y \Delta y$		x-y coupl
X		$\Delta B_x = 2B'' x \Delta y$		x-y coupl

Φ_b = bend angle of DIP, ρ = bend radius of DIP
L = lengths of Quad, $K^2 = B' / B \rho$

In combined function magnets, all of the above sources of closed orbit errors have to be considered. Furthermore, due to the large bending angle, there is a mixing of misalignments as will be shown in section-3.

The effect of misalignments of the magnets on the closed orbit is usually calculated by modeling programs, such as MAD, SYNCH, PETROC, etc. In order to follow the orbit in the magnet it is necessary to "cut" the magnet into **n** segments and calculate the misalignment of each of these sections assuming a given misalignment of the whole magnet. These calculations will be presented in section-3 and their application to the SXLS ring [1] in section-4.

4. MISALIGNMENT OF A SEGMENT OF LARGE BEND-ANGLE MAGNETS

4.1 Definitions and notations

The magnet will be considered as consisting of **n** identical segments of $\alpha = \Phi_b/n$ bending angle each.

MAD requires the specification of the misalignment of a magnet in terms of the ΔX, ΔY, ΔZ misplacements and Θ_x (pitch), Θ_y (yaw), Θ_z (roll) rotations between the reference orbit and the normal vectors of the magnet in the **beam's local coordinate system.** In this coordinate system the direction of the z-axis coincides with the direction of the beam, the x-axis is in and the y-axis is perpendicular to the orbital plane. Their direction is specified by the right handedness of the coordinate system.

A few notations and definitions are introduced here. The intersection of the reference orbit with the entry face of the i-th segment will be called **center point,** P_i. The center point of the misaligned segment will be denoted by P'_i. The magnet's or a segment's **own coordinate system** is the beam's local coordinate system with the origo at P or at P_i. This means, that the $\vec{u}$, $\vec{v}$, $\vec{t}$ normal (unit) vectors of the entry face of the magnet lie on the x, y, z-axes (see Fig. 1). ΔX, ΔY, ΔZ, Θ_x, Θ_y, Θ_z will refer to the misalignments of the whole magnet in its X,Y,Z coordinate system, while Δx_i, Δy_i, Δz_i, $\theta_{x,i}$, $\theta_{y,i}$, $\theta_{z,i}$ refer to the misalignments of the i-th segment in their x_i, y_i, z_i coordinate systems. For convenience, on the following figures Φ_b = 180° and n = 6 are used.

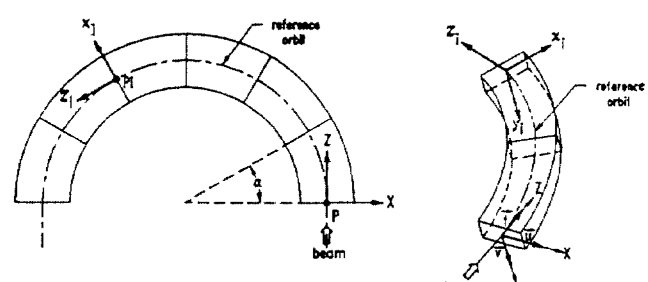

Fig. 1
Definition of the X,Y,Z and x_i, y_i, z_i coordinate systems.

The 1-st segment's own coordinate system, (x_1, y_1, z_1), is identical with that of the whole magnet, (X,Y,Z). Because of the choice of the origo, the Δx_i, Δy_i, Δz_i misplacements of the i-th segment are the x_i, y_i, z_i coordinates of the P'_i point. Roll, pitch and yaw are defined by the θ_z, θ_x and θ_y angles between $(\vec{u}, \vec{u}')$ as projected on the (x,y)-plane, $(\vec{t}, \vec{t}')$ as projected on the (y,z)-plane and $(\vec{t}, \vec{t}')$ as projected on the (z,x)-plane, respectively (see Figs. 2).

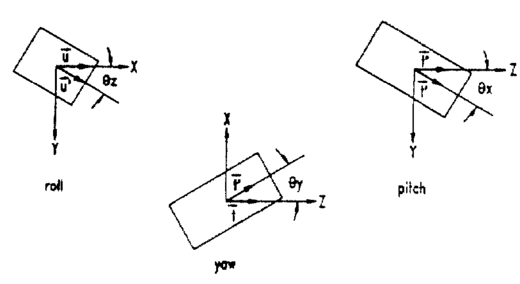

Figs. 2
Definition of roll, pitch and yaw.

[+]Work performed under the auspices of the U.S. Department of Energy and funded by U.S. DoD.

* For replacing truly extended kicks with a point kick, see ref. [5].

4.2 ΔX misplacement

The whole magnet is misplaced by ΔX. This is a two-dimensional problem, mixing the Δx_i and Δz_i misplacements as shown on Fig. 3. It is easy to see, that Δx_i and Δz_i for the i-th segment can be calculated as

$$\Delta x_i = \Delta X \; cos[(i-1)\alpha] \quad \text{and} \quad \Delta z_i = -\Delta X \; sin[(i-1)\alpha] \qquad (2)$$

4.3 Yaw

The whole magnet is rotated by Θ_y around the Y-axis. This is a two-dimensional problem, mixing the $\theta_{y,i}$ rotations and the Δx_i, Δz_i misplacements as shown on Fig. 4.

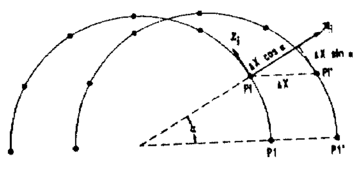

Fig. 3
ΔX misplacement of the 180° magnet

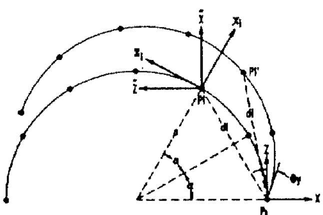

Fig. 4
Θ_y yaw of the 180° magnet

The yaw of each segment are identical: $\theta_{y,i} = \Theta_y$. The Δx_i, Δz_i misplacements are calculated as follows.

The coordinates of P_i and P'_i are first calculated in the (X,Z) coordinate system:

$$X^{P_i'} = d_i sin[(i-1)\frac{\alpha}{2} - \Theta_y], \qquad X^{P_i} = d_i sin(i-1)\frac{\alpha}{2},$$

$$Z^{P_i'} = d_i cos[(i-1)\frac{\alpha}{2} - \Theta_y], \qquad Z^{P_i} = d_i \cos(i-1)\frac{\alpha}{2},$$

where d_i is the sagitta, given by $d_i = 2\,\rho\,\sin[(i-1)\frac{\alpha}{2}]$.

After applying coordinate transformation from (X,Y) to $(\tilde{X},\tilde{Y})$ by mooving the P_1 origo to P_i one obtains for small Θ_y's (such that $\cos\Theta_y \approx 1$ and $\sin\Theta_y \approx \Theta_y$:

$$\tilde{X}^{P_i'} = X^{P_i'} - X^{P_i} \approx -d_i \Theta_y \cos(i-1)\frac{\alpha}{2} = -\rho\Theta_y \sin(i-1)\alpha,$$

$$\tilde{Z}^{P_i'} = Z^{P_i'} - Z^{P_i} \approx \; d_i \Theta_y \sin(i-1)\frac{\alpha}{2} = \rho\Theta_y\,[1 - \cos(i-1)\alpha].$$

Finally, applying a coordinate rotation by $(i-1)\alpha$, the coordinates of P_i' are obtained in its own, (x_i,z_i), coordinate system (which are in fact, the misplacements of the i-th segment):

$$\Delta x_i \equiv x_i^{P_i'} = -\tilde{Z}^{P_i'}\sin(i-1)\alpha + \tilde{X}^{P_i'}\cos(i-1)\alpha = -\rho\Theta_y \sin(i-1)\alpha \qquad (3a)$$

$$\Delta z_i \equiv z_i^{P_i'} = \tilde{Z}^{P_i'}\cos(i-1)\alpha + \tilde{X}^{P_i'} sin(i-1)\alpha = -\rho\Theta_y\,[1 - cos(i-1)\alpha] \qquad (3b)$$

4.4 Roll

The whole magnet is rotated by Θ_z angle around the z-axis. This is a three dimensional problem mixing the Δy_i misplacement and the $\theta_{x,i}$, $\theta_{z,i}$ rotations as shown on Fig. 5. It can be seen, that the Δx_i, Δy_i

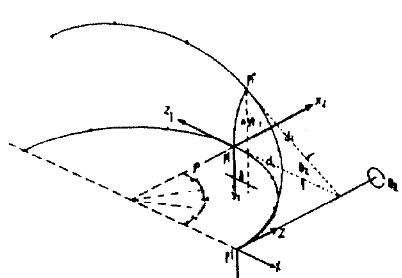

Fig. 5
Θ_z roll of the 180° magnet

misplacements of the i-th segment are:

$$\Delta x_i = \Delta\,[sin(i-1)\alpha], \quad \Delta z_i = \Delta\,[cos(i-1)\alpha], \quad \text{and} \quad \Delta y_i = d_i \sin\Theta_z,$$

$$where \quad \Delta = d_i[1 - cos\,\Theta_z], \quad \text{and} \quad d_i = \rho[1 - cos(i-1)\alpha].$$

For realistically small misalignments ($\Theta_z \leq 1$ mrad), this yields:

$$\Delta x_i \approx \Delta z_i \approx 0, \quad \text{and} \quad \Delta y_i \approx d_i \Theta_z = \Theta_z \rho[1 - cos(i-1)\alpha]. \qquad (4a)$$

The pitch of the i-th segment, θ_{x_i}, is the projection of the $(\vec{t_i}, \vec{t_i}')$ angle on the (y_i,z_i) plane, while the roll, θ_{z,i_i}, is the projection of the $(\vec{u_i}, \vec{u_i}')$ angle on the $(x_{i,}y_i)$-plane. Remembering, that the original roll of the whole magnet, Θ_z, is the $(\vec{u}_1, \vec{u}_1')$ angle, which is the same as the projection of the $(\vec{u}_1, \vec{u_i}')$ angle on the (x_1,y_1)-plane, one can get:

$$tg\,\theta_{x,i} = sin(i-1)\alpha \; tg\,\Theta_z \approx \Theta_z \sin(i-1)\alpha, \qquad (4b)$$

$$tg\,\theta_{z,i} = cos(i-1)\alpha \; tg\,\Theta_z \approx \Theta_z \cos(i-1)\alpha. \qquad (4c)$$

4.5 Pitch

The whole magnet is rotated by Θ_x angle around the x-axis. This is a three dimensional problem mixing the Δy_i misplacement and the $\theta_{x,i}$, $\theta_{z,i}$ rotations as shown on Fig. 6. The misplacements of the i-th

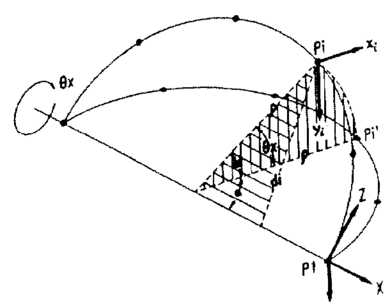

Fig. 6
Θ_x pitch of the 180° magnet

segment are (for small Θ_x):

$$\Delta x_i \approx 0, \quad \Delta y_i \approx d_i \Theta_x = \Theta_x \rho \sin(i-1)\alpha.$$

The rotations can be calculated similarly to section-3.4, except that the role of $\theta_{x,i}$ and $\theta_{z,i}$ are reversed.

$$\theta_{x,i} \approx \Theta_x \cos(i-1)\alpha, \quad \theta_{z,i} \approx \Theta_x \sin(i-1)\alpha.$$

5. RESULTS

Closed orbit errors were calculated for the SXLS ring. This is a two-superperiod, 200 Mev ring of C=8.5 m circumference. Each superperiod consists of a 180° combined function magnet with bending radius of ρ=0.6 m and two additional short ($l \approx 0.15$ m) quadrupoles, as indicated on Fig. 7. The horizontal and vertical tunes are ν_x=1.415, ν_y=0.415, and consequently, the horizontal and vertical phase advances accross the magnet are $\phi_x \approx 180°$ and $\phi_y \approx 18°$, respectively. The β_x, β_y and η_x machine functions are shown on Fig. 7.

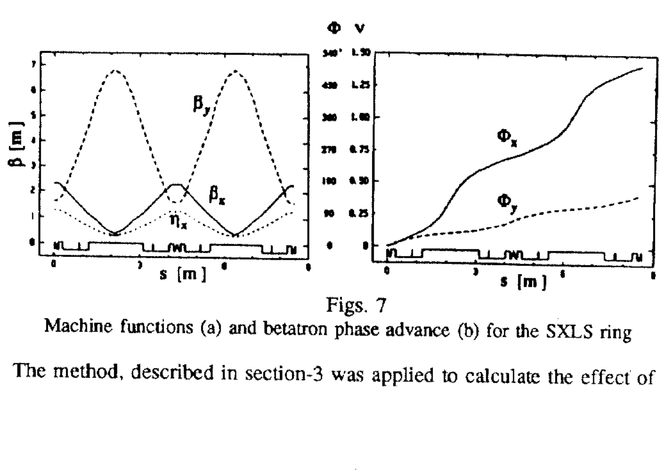

Figs. 7
Machine functions (a) and betatron phase advance (b) for the SXLS ring

The method, described in section-3 was applied to calculate the effect of a given misalignment of the bending magnets. Figs. 8a and b show the distorted horizontal closed orbit, x_{co} as a result of a ΔX = 1 mm misplacement and Θ_y = 1 mrad yaw of one of the bending magnet. The so-

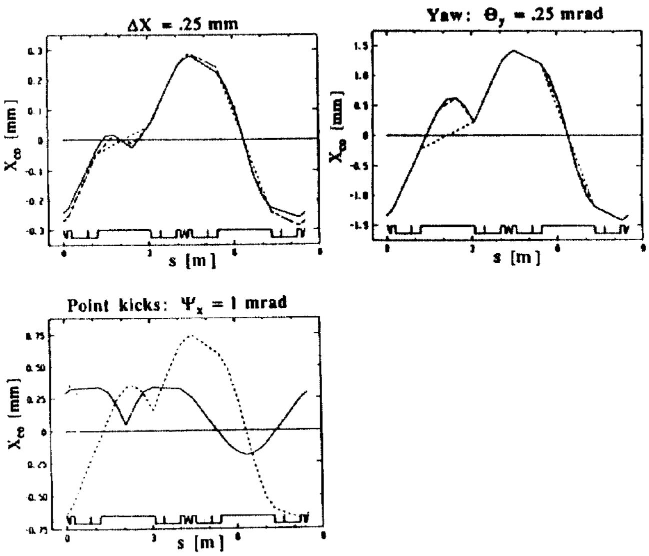

Figs. 8
Horizontal closed orbit errors due to ΔX, Θ_y misalignments and Ψ_x kick at the middle (solid curve) and at the end (broken curve) of the magnet

lid curves correspond to n=6, while the broken and dotted curves were calculated with n=3 and 1, respectively. It is interesting to note, that the ΔX and Θ_y misalignments of the magnet yield distorted closed orbit of very similar shape but strongly different magnitude. The same shape of orbit results from a point kick at the exit end of the magnet (but not at the middle of the magnet since the kick approximation of equ.(1) is not valid) as shown on Fig. 8c. Point kick at the end of the magnet may result from deviation of the actual from the design fringe field.

On Fig. 9a ,b and c the distorted vertical closed orbit, y_{co}, is shown as a result of a ΔY=-1 mm displacement, Θ_z=1 mrad roll and Θ_x=1 mrad pitch, respectively.

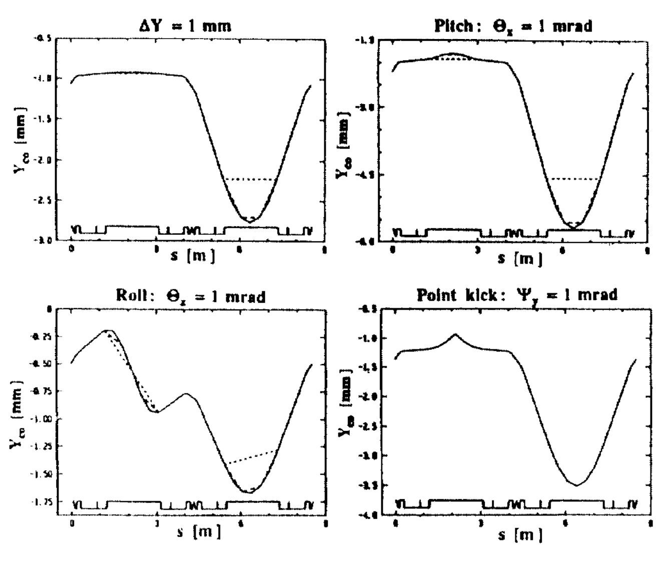

Figs. 9
Vertical closed orbit errors due to ΔY, Θ_z, Θ_x misalignments and Ψ_y kick at the middle of the magnet

It can be seen the ΔY, Θ_x and Θ_z misalignments (especially the former two), yield closed orbits of a similar shape and different magnitude. This is due to the fact, that because of the small vertical phase advance accross the magnet, the point kick approximation of equ.(1) is valid. This point is further illustrated by comparing the orbits on Figs. 9a-c with the closed orbit resulting from a Ψ_y=1 mrad kick at the middle of the magnet as shown on Fig. 9d.

The largest closed orbit distortions are caused by the Θ_y and Θ_x rotations of the magnet. In all cases, however, since the misalignment of the magnet can easily be kept under 0.25 mm and 0.25 mrad, the maximum closed orbit errors are:

$$|x_{co}^{max}| \le 0.35mm, \quad x_{co}^{peak-to-peak} \le 0.7mm \quad |x'^{max}_{co}| \le 0.4mrad$$
$$|y_{co}^{max}| \le 1.4mm, \quad y_{co}^{peak-to-peak} \le 0.9mm \quad |y'^{max}_{co}| \le 0.6mrad$$

Unlike in large rings with many magnets, where their misalignment is random, the two 180^o magnet can be misaligned either in the same or in the opposite sense. The results are shown on Figs. 10 for two representative cases, yaw and pitch.

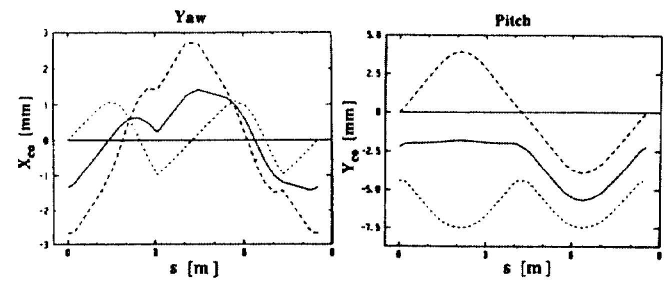

Fig.10
The effect of +1 mrad misalignment in one dipole (solid lines) or in both dipoles (broken lines) and +1, -1 mrad in the two dipoles (dotted lines)

For the realistic 0.25 mm and 0.25 mrad misalignments, the maximum closed orbits errors due to misalignments of both bending magnets are:

$$|x_{co}^{max}| \le 0.7mm, \quad x_{co}^{peak-to-peak} \le 1.4mm, \quad |x'^{max}_{co}| \le 0.8mrad$$
$$|y_{co}^{max}| \le 1.9mm, \quad y_{co}^{peak-to-peak} \le 1.0mm, \quad |y'^{max}_{co}| \le 0.6mrad$$

Detailed analysis of the closed orbit errors and correction scheme is given in [6].

ACKNOWLEDGEMENT
The author is indebted to Jim Niederer and Chris Iselin for many discussions on the subject and to Sal Pjerov for his careful work on producing the figures.

REFERENCES

1. J.B.Murphy: X-ray Lithography Sources; a Review, Proc. of the IEEE Particle Accelerator Conf., Vol.2, p.757, 1989.
2. D.E. Andrews et al.: A Compact Synchrorton X-ray Source for X-ray lithography, AIP Conf. Proc. No 171, p.135, 1988.
3. N. Takahashi: Compact Superconducting SR ring for X-ray Lithography, NIM B24/25 p.425, 1987.
4. T. Hosokawa et al.: NTT Supercunducating Storage Ring - Super ALIS, 3-rd Int. Conf. on SR Instrumentation, Japan, 1988.
5. S. Krinsky: Closed orbit distortion resulting from an extended kick, NSLS Tech. Note #14, 1978.
6. Eva Bozoki: Closed orbit errors and correction in the SXLS ring, BNL- report, in preparation.